New Class of Instabilities in Passive Optical Cavities

D. W. McLaughlin, J. V. Moloney, and A. C. Newell
Applied Mathematics Program and Optical Science Center, University of Arizona, Tucson, Arizona 85721
(Received 2 July 1984)

In this Letter we show that the fixed points of the Ikeda map are more unstable to perturbations with a short-scale transverse structure than to plane-wave perturbations. We correctly predict the most unstable wavelength, the critical intensity, and the growth rates of these disturbances. Our result establishes that, for a large class of nonlinear waves, spatial structure is inevitable and drastically alters the route to chaos. In an optical cavity the consequence is that the period-doubling cascade is an unlikely scenario for transition to optical chaos.

PACS numbers: 42.65.–k

In this Letter, we announce a new and unexpected result, an instability whose consequences have ramifications for a large class of nonlinear wave problems whose dynamics can be described by envelope equations. Specifically, it deals with periodically forced field equations of the universal nonlinear Schrödinger type. This instability changes the whole character of the route of the system from a simple to a turbulent state. It generates spatial structure, and the subsequent onset of chaotic behavior completely bypasses the period-doubling scenario which is relevant if spatial structure is ignored. Moreover, the scenario which does emerge has a universal character of its own. Examples of this phenomena are found in optics, either in the transmission along optical fibers or in optically bistable cavities.[1] It is in the latter context that this work is presented.

In this problem we are interested in the long-time state of a continuous laser signal which is recirculated through a nonlinear medium. In examining one particular manifestation of optical bistability (a ring cavity with Kerr nonlinearity), Ikeda[2] wrote a map expressing the (complex) amplitude g_{n+1} of the electric field **E** on the $(n+1)$st pass through the cavity as a function of electric field amplitude on the nth pass;

$$g_{n+1} = a + Rg_n \exp[i\phi_0 + ipLN(I)/2]. \quad (1)$$

In (1), a is the amplitude of the input field, $R < 1$ the reflectivity of the mirrors, ϕ_0 the detuning parameter, p is (effectively) the length of the nonlinear medium, and $N(g_n g_n^*)$ measures its nonlinear response. Two cases are usually studied: (1) the saturable medium, $N(I) = -(1+2I)^{-1}$, (2) the Kerr medium, $N(I) = -1+2I$, which is the small intensity limit of the saturable case. Equation (1), called the Ikeda map, is a two-dimensional invertible map and exhibits a variety of behavior which is already well documented in the literature.[2–4] In various parameter ranges (the two parameters which are varied are a and p), one finds multiple fixed points (see Fig. 1) and sequences of period-doubling bifurcations leading to chaotic attractors.

The map (1) invokes the plane-wave approximation in which diffraction effects are neglected. The purpose of this Letter is to point out that this assumption is not justified even for cases in which the input beam is very slowly varying in the transverse direction $\mathbf{x}(x,y)$ and the Fresnel number is large. The reason is that the fixed point solutions of the plane-wave map (1) are more unstable to perturbations with a short-scale transverse structure than they are to perturbations with plane-wave structure. To emphasize this point, the numerical experiment discussed in this Letter is run at a parameter value p for which the fixed points of the Ikeda map are stable!

This discovery has important ramifications. First, it shows that the initial bifurcation of the system introduces an extra dimension into the problem, a short-wave transverse excitation of temporal period two. This extra dimension affects significantly the subsequent behavior of the system. As the stress parameters are raised, no period-doubling cascades into chaos

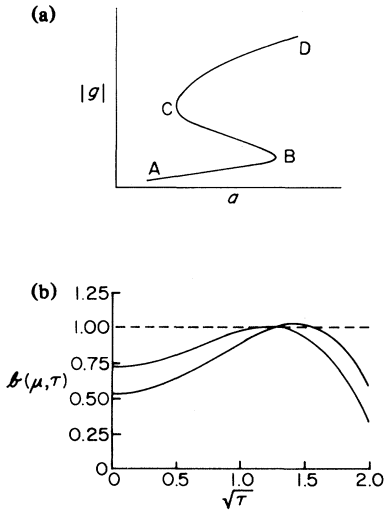

FIG. 1. (a) The multivalued response of the amplitude of the fixed point $|g|$ vs a at fixed values of p for the Ikeda map. (b) A graph of $b(\mu,\tau)$ vs $\sqrt{\tau} = \sqrt{\gamma}K$ for $\mu = pI = pgg^*$ equal to 0.11 and 0.24.

are observed. Instead, chaotic behavior arises as a temporally irregular sharing of energy between the short-wave transverse structure and a long wavelength background. This modulation causes the system to drift back towards its original fixed point (at which the amplitude of the short-wave transverse excitation is zero) which, for these parameter values, is an unstable saddle point. It is the sensitive behavior of the system in this neighborhood that gives rise to a modulational and intermittent chaotic behavior.

Second, these findings show that in nonlinear passive cavities transverse spatial structure is inevitable. It had previously been noted[5] that if the amplitude of the input Gaussian were to exceed a value corresponding to the point B in Fig. 1(a), then part of the signal would switch to the upper branch CD and part would remain on the lower branch AB thereby creating large gradients in the electric field envelope and making diffraction important. In this Letter, we have chosen values of the input intensity so that one is always on the lower branch AB of Fig. 1(a). In this case, it is the high transverse wave-number instability which makes the diffraction term important. It turns out that the most unstable wave number which the dynamics chooses is always such that diffraction is as important as nonlinearity. In this respect, the instability is reminiscent of the Benjamin-Feir[6] or modulational instability which is so widespread in physics. While the two instabilities arise from two different mechanisms, they should share the property of ubiquity.

The Ikeda map arises by combining the equation for the propagation of the electric field envelope $G_n(\mathbf{x},z)$ on the nth pass around a nonlinear medium in the shape of a rectangular circuit of length L $(0<z<L)$

$$2iG_{nz}+\gamma\nabla^2 G_n+pN(G_nG_n^*)G_n=0, \tag{2}$$

with the boundary condition which gives the starting profile $G_{n+1}(\mathbf{x},0)$ in terms of the input field envelope $A(\mathbf{x})$ and the value of the electric field envelope $G_n(\mathbf{x},L)$ at the end of the nth pass,

$$G_{n+1}(\mathbf{x},0)=\sqrt{T}A(\mathbf{x})+Re^{i\phi_0}G_n(\mathbf{x},L). \tag{3}$$

In (2), the parameter $\gamma=\ln 2/4\pi F$, where F is the Fresnel number and $T=1-R$ is the transmission coefficient.

Observe that the Ikeda map (1) is obtained by assuming that both $\sqrt{T}A(\mathbf{x})=a$ and the response $G_n(\mathbf{x},z)$ are $\mathbf{x}$ independent. Usually the stability of fixed points of (1) is studied with respect to perturbations with no transverse structure, yielding period-doubling cascades, etc.[4]

However, the class of allowable perturbations is much broader and includes modes with an $\mathbf{x}$-dependent spatial structure. Our study of these proceeds in two parts: (i) Using a linearization we compute the most unstable spatial wavelength; (ii) we adapt the results of this linearization to a numerical experiment whose input envelope has a Gaussian profile and compute the growth rate and threshold intensity of the instability. The linearization (i) begins by setting

$$G_n(\mathbf{x},z)=[|g|+y_n(\mathbf{x},z)]\exp[\tfrac{1}{2}ipN(I)z+i\arg g], \quad I=gg^*,$$

in (2), calculate the $(\mathbf{x},z)$ structure of $y_n(\mathbf{x},z)$ from (2) and use the solution in the map (3). The algebra is straightforward and one finds

$$y_n(\mathbf{x},z)=e^{i\nu z}(a_ne^{i\mathbf{K}\cdot\mathbf{x}}+b_ne^{-i\mathbf{K}\cdot\mathbf{x}})+e^{-i\nu z}(c_ne^{i\mathbf{K}\cdot\mathbf{x}}+d_ne^{-i\mathbf{K}\cdot\mathbf{x}})$$

for $4\nu^2=\gamma^2K^4-2p\gamma N'(I)IK^2>0$, and $K^2=K_x^2+K_y^2$. The coefficients a_n, b_n, c_n, and d_n are related, i.e.,

$$-pN'(I)Id_n^*=[-2\nu-\gamma K^2+pN'(I)I]a_n, \quad -pN'(I)Ib_n^*=[2\nu-\gamma K^2+pN'(I)I]c_n.$$

Since I is small on the lower branch, we can use the Kerr approximation and write $N(I)=-1+2I$. The map (3) can be written $y_{n+1}(\mathbf{x},0)=Re^{i\phi}y_n(\mathbf{x},L)$, $\phi=\phi_0+\frac{1}{2}pLN(I)$, which gives $(a_{n+1},c_{n+1})^T=M(a_n,c_n)^T$, with

$$M=R\begin{pmatrix} e^{i\nu L}(\cos\phi+i\beta\sin\phi) & ie^{-i\nu L}(i-\beta)\sin\phi \\ ie^{i\nu L}(i+\beta)\sin\phi & e^{-i\nu L}(\cos\phi-i\beta\sin\phi)\end{pmatrix}$$

where $2\nu\beta=2\mu-\tau$, $\tau=\gamma K^2$, and $\mu=pI$. Looking for solutions $(a_n,c_n)^T=(-1)^n\rho^n(a,c)^T$, we find $\rho^2-2b\rho R+R^2=0$ where $2Rb=TrM$. The potentially unstable root is $\rho/R=b+(b^2-1)^{1/2}$ where

$$b(\mu,\tau)=\cos(\psi+\mu)\cos\nu+[(\tau-2\mu)/2\nu]\sin(\psi+\mu)\sin\nu$$

with $\psi=\pi+\phi_0-\frac{1}{2}p$, $2\nu=(\tau^2-4\mu\tau)^{1/2}$ and we have set $L=1$ without loss of generality. The case $\nu^2=-\sigma^2<0$, i.e., $\tau<4\mu$, is realized by an analytic continuation $\nu=-i\sigma$ and the stability with respect to plane-wave perturbations can be investigated by setting $K=0$, whence $b(\mu,0)=\cos(\psi+\mu)-\mu\sin(\psi+\mu)$. The stability threshold (i.e., $\rho=1$) is reached when $b=b_c=\frac{1}{2}(R+1/R)$. In Fig. 1(b) we display the graphs of $b(\mu,\tau)$ for two values of $\mu=0.11$, 0.24. We observe the following: (1) As τ increases from zero, $b(\mu,\tau)$ increases and reaches a maximum at a unique value of $\tau=\gamma K^2$. The value $\mu=\mu_c=0.11$ is the lowest value of the intensity $\mu=pI$ for which

period doubling can occur. (2) For $\mu = 0.24$, there is a narrow band $(1.29 < \tau < 1.55)$ of unstable wave numbers. The one with the maximum growth rate is $\tau = 1.43$. For $\gamma = 1.67 \times 10^{-3}$, this corresponds to a wavelength of $\lambda = 2\pi/K = \sqrt{\gamma}\,2\pi/\sqrt{\tau} = 0.21$. (3) For these parameter values, the most unstable wave number lies outside the Benjamin-Feir unstable band, $\tau < 4\mu$. In this band, the signal is amplified as it propagates down the nonlinear medium and should the most unstable wave number lie in this range, the amplification per pass is significantly increased. The function $b(\mu, \tau)$ was also drawn as function of τ for several different situations, and the following observations were made: (1) $b(\mu, 0) < b_c$ for all values of μ, consistent with the result obtained in Ref. 4 that, for $p = 6$, no period doubling of the Ikeda map occurs. (2) The defocusing case, $p\gamma < 0$; for $p = -6$, $\phi_0 = -0.4$, $\psi = -\pi + \phi_0 - \frac{1}{2}p$, which is the symmetric counterpart of Fig. 1(b), $b(\mu, \tau)$ begins from the same value at $\tau = 0$ but then decreases. For these parameters, all modes are stable, but $K = 0$ is the least stable. (3) However, short-scale transverse instabilities can occur even in the defocusing case. For example, for $p = -9$, the critical intensity μ is less for finite K modes, although generally the values of the intensity at which period doubling occurs are greater if the medium is defocusing $(p\gamma < 0)$ than when it is focusing $(p\gamma > 0)$.

Finally, we give the results of a numerical experiment in which only one transverse dimension x was used. The experiment was carried out with the use of an input beam whose envelope $\sqrt{T}A(x)$ has a Gaussian profile, which is a more accurate model for real experiments. Because the width of the Gaussian is several times greater than the wavelength of the most unstable transverse fluctuation, a WKB (geometrical optics) approach is valid, and, to leading order, agrees with the results obtained by assuming the unperturbed solution $g(x)$ [obtained by solving (1) for the fixed point with $a = a(x)$] to be locally constant. We will correctly predict the critical wavelength and critical intensity. The postbifurcation evolution of the period-doubled transverse fluctuation requires one to consider the loss of energy from the center of the beam to the wings in addition to the energy input to the fluctuation from instability. Therefore, in order to sustain the growth in the middle part of the beam, the intensity μ (which is proportional to the input intensity a) has to be sufficiently greater than μ_c [the value at which disturbances can possibly grow if $a(x)$ were constant] in order to offset this radiation loss.

Figure 2 shows the electric field envelope after (a) 120 passes at which time the system is very close to its (weakly) unstable fixed point (in function space) and (b) an overlay of the output data for passes $n = 260$–280 inclusive at which stage one can observe

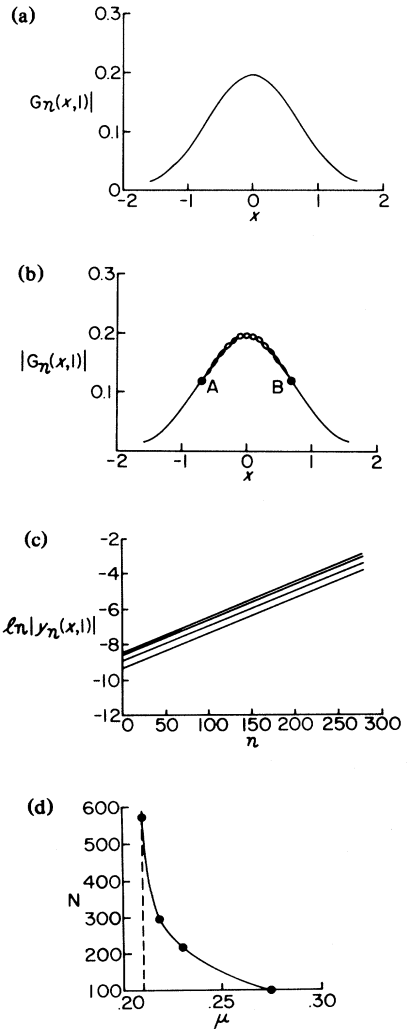

FIG. 2. (a) The (weakly) unstable fixed point; i.e., the solution of (2) and (3) for $\gamma = 1.67 \times 10^{-3}$, $p = 6$, $\phi_0 = 0.4$, and $\sqrt{T}A(x) = 0.12\exp(-x^2)$ after 120 passes. (b) An overlay of the output for passes $n = 260$ to 280 which alternates on successive passes between the two interwoven graphs. The wavelength of the fluctuation at the crest, which is equal to the distance between crests of either one of the interwoven strands, is 0.21. The points A and B correspond to values of $\mu = 0.117$. (c) The growth of the logarithms of the amplitudes of the transverse perturbation as a function of n at the four locations $x = 0, 0.18, 0.37, 0.55$. (d) The number of passes vs μ required for the instability to reach a prescribed amplitude.

that the transverse perturbation has begun to grow. Observe the period-two temporal character of the growing perturbation. The wavelength of the perturbation (the distance between two successive crests on even or odd passes) at the maximum is 0.21 which is

exactly as predicted by theory. We also verified the critical wavelength at $\mu = 0.26$ is 0.22, again as predicted by theory. We observe in Fig. 2(b) that the perturbations initially grow of their own accord down to amplitudes of 0.13 which corresponds to a value of μ of $pI = 6(0.14)^2 = 0.117$, again in close agreement with theory.

In order to compute the effective growth rate per pass, we calculate the energy input to and loss from the region AB of Fig. 2(b). The rate of energy change per pass per unit length is

$$\frac{\delta E}{E} = \frac{1}{AB}\left[\int_{AB} \delta\rho(x)\,dx - \frac{2}{K}\frac{\tau - 2\mu}{(1-4\mu/\tau)^{1/2}}\right] \quad (4)$$

where the first term is the energy gained in the excited region AB and the second is that lost through being carried out of the region at a rate measured by the group velocity of the most excited wave in the packet. The result is 0.04. Therefore, the percentage increase in amplitude is 0.02. In Fig. 2(c), we draw the graphs of the logarithms of the amplitudes at various stations $x = 0, 0.18, 0.37, 0.55$ [in Fig. 2(b)] and observe that in each case the growth rate is indeed 0.02.

Finally, we compute the effective critical intensity μ_e, namely, that value of μ corresponding to the maximum of the profile in Fig. 2(b), for which the right-hand side of (4) is zero. We predict $\mu_e = 0.205$. In Fig. 2(d) we draw the number of passes needed to observe the instability (in other words, for its amplitude to grow to a certain amount) versus μ. Note that the curve is asymptotic to a value of $\mu = 0.205$.

The purpose of this Letter has been to demonstrate how transverse fluctuations and diffraction effects are inevitable in passive linear cavities. Because these modes arise as instabilities, they simply cannot be removed by an appropriate tailoring of the input profile. The subsequent development of these lower-branch instabilities and their role in causing modulational chaos will be discussed in a review paper.[7] The two-dimensional degeneracy of these unstable modes (observe that the wave number γK^2, and not its direction $\mathbf{K}$, is chosen by dynamical considerations) also offers a challenge to the theoretician. It is not yet clear under what circumstances in a two-transverse-dimension medium that circular rings, independent of the azimuthal direction, will be the favored mode of oscillation for amplitudes on the lower branch.

The authors are grateful for support from the following: the Air Force Office of Scientific Research (AFOSR Contract No. PR-83-00869), the Army Research Office (ARO Contract No. DAAG29-81-K-0025), and the Office of Naval Research (ONR Contract No. N00014-84-K-0420). We also thank E. A. Overman for his help with numerical calculations.

[1] *Optical Bistability,* edited by C. M. Bowden, M. Ciftan, and H. R. Robl (Plenum, New York, 1981); *Optical Bistability II,* edited by C. M. Bowden (Plenum, New York, 1984).

[2] K. Ikeda, H. Daido, and O. Akimoto, Phys. Rev. Lett. **45**, 709 (1980); K. Ikeda, Opt. Commun. **30**, 257 (1979).

[3] R. R. Snapp, H. J. Carmichael, and W. C. Schieve, Opt. Commun. **40**, 68 (1981); H. J. Carmichael, R. R. Snapp, and W. C. Schieve, Phys. Rev. A **26**, 3408 (1982); W. J. Firth, Opt. Commun. **39**, 343 (1981).

[4] J. V. Moloney, Opt. Commun. **45**, 435 (1984).

[5] J. V. Moloney and H. M. Gibbs, Phys. Rev. Lett. **48**, 1607 (1982); D. W. McLaughlin, J. V. Moloney, and A. C. Newell, Phys. Rev. Lett. **51**, 75 (1983).

[6] T. B. Benjamin and J. E. Feir, J. Fluid Mech. **27**, 417 (1966).

[7] D. W. McLaughlin, J. V. Moloney, and A. C. Newell, to be published.